Novel Synthesis Pathway of ZnO Nanoparticles from the Spontaneous Hydrolysis of Zinc Carboxylate Salts

Geonel Rodríguez-Gattorno,[†] Patricia Santiago-Jacinto,[‡] L. Rendon-Vázquez,[‡] József Németh,[§,||] Imre Dékány,[§,||] and David Díaz*[,†]

Departamento de Química Inorgánica y Nuclear, Facultad de Química, Universidad Nacional Autónoma de México, Coyoacán, 04510, México D.F., México, Departamento de Materia Condensada, Instituto de Física, Universidad Nacional Autónoma de México, Coyoacán, 04510, México D.F., México, Department of Colloid Chemistry, University of Szeged, H-6720 Szeged, Hungary, and Nanostructured Materials Research Group of the Hungarian Academy of Science, H-6720 Szeged, Hungary

Received: June 23, 2003; In Final Form: August 28, 2003

A novel and easy synthesis pathway to synthesize small ZnO nanoparticles with a narrow size distribution is reported. The synthesis implies the simple dissolution of a zinc carboxylate hydrated salt (cyclohexanebutyrate or acetate) in a polar basic aprotic solvent as dimethyl sulfoxide (DMSO) or *N*,*N*′-dimethylformamide (DMF) at room temperature. It is necessary to control the water content and temperature to ensure the reproducibility. The hydrolysis of zinc carboxylates allows the formation of ZnO nanoparticles of different sizes, depending on reaction conditions. Solvent basicity and the interaction of DMSO−H_2O play crucial roles on the hydrolysis mechanism. The stability and the optical properties of the ZnO colloids were monitored by UV−visible electronic absorption and emission spectroscopies. From an HR-TEM study it was established that low concentration (2×10^{-4} M) of zinc cyclohexanebutyrate and zinc acetate afforded ZnO nanocrystallites of (2.12 nm, SD = 0.76) and (3.0 nm, SD = 0.5), average size, respectively. ZnO nanocrystals with rock salt structure coexist with wurtzite structure when zinc cyclohexanebutyrate is used as the starting salt. Dynamic light backscattering size measurements of ZnO nanoparticles were accomplished in DMSO colloid dispersions, resulting in the detection of small individual nanoparticles and assemblies of nanoparticles. Powder X-ray diffraction spectroscopy was used to accomplish the nanoparticle characterization, of DMF dispersions. Experimental results show that cyclohexanebutyrate acts as a more effective capping agent than acetate. Low concentration (2×10^{-4} M) colloidal ZnO dispersions in DMSO did not show any flocculation or red shift in two months, probably due to the concatenated dynamic stabilizing action of carboxylate ions and solvent molecules. The ZnO colloids in DMF are not stable and readily precipitate; moreover, nanoparticles in this solvent tend to adhere to glass walls, which allows production of ZnO films.

Introduction

Very few semiconductors have so many applications as ZnO and TiO_2. Rubber products, ceramics, paints, pharmaceutical, and agricultural applications are the main uses of the bulk zinc oxide, while ZnO nanoparticles (NPs) have been receiving much attention in recent years due to potential and established technological applications, among those that can be cited solar energy conversion,[1] photocatalysis for partial or total mineralization of organic compounds,[2] nonlinear optics,[3] gas sensors,[4] UV-blockings,[5] and light-emitting materials.[6]

The sol−gel method,[7,8] phase transfer technique,[9] hydrolysis of chelate complex,[10] polymer stabilization,[11] and alkoxide-based processes[12] are some examples of reported colloidal approximation to obtain ZnO nanoparticles. In addition, other methods such as low-pressure chemical vapor deposition,[13] atomic layer deposition[1], thermal decomposition of precursors,[14] spray pyrolysis,[15] and laser heating[16] have been used to produce ZnO nanoparticles and thin films.

New routes that involve a minimum number of components in colloidal synthesis are welcome, avoiding undesirable excess of starting compounds, parallel reactions, and byproducts that finally contaminate the dispersions. Mullenkamp[17] has paid attention to the importance of having pure colloidal dispersions as the first step toward device fabrication, allowing clean film preparations and unambiguous optical response interpretations.

Dimethyl sulfoxide (DMSO) and *N*,*N*′-dimethylformamide (DMF) have been demonstrated to be very useful solvents in nanoparticle preparation. Their high dielectric constants[18] allow charge separation; turning them into good solvents for ionic solids and polar and polarizable molecules.[19] Their chemical properties assist to induce photochemical reactions that are not possible in other solvents.[20,21] Very stable nanoparticle dispersions in DMSO and DMF have been previously reported.[22−25] Díaz and coauthors[26] and Elbaum et al.[27] have also shown a very simple pathway for the spontaneous formation of metallic silver and CdS nanoparticles, in which DMSO plays a decisive role in the synthesis mechanism and as an important stabilizing agent.

* Corresponding author. Phone/fax: 52-55-5622-3813. E-mail: david@servidor.unam.mx

[†] Departamento de Química Inorgánica y Nuclear, Universidad Nacional Autónoma de México.

[‡] Departamento de Materia Condensada, Universidad Nacional Autónoma de México.

[§] University of Szeged.

[||] Nanostructured Materials Research Group.

10.1021/jp035788x CCC: $25.00
Published on Web 10/29/2003

The main aims and novelty of this work are to report a new, direct, clean, and very easy pathway to obtain ZnO nanoparticles with narrow size distribution by simple dissolution of a zinc carboxylate salt (acetate or cyclohexanebutyrate) in a polar basic aprotic solvent as DMSO or DMF. The resulting colloidal dispersions of ZnO NPs in DMSO, of low concentrations, are stable for at least two months. Experimental results show unambiguously that the cyclohexanebutyrate anion acts as a more efficient capping agent than the acetate ion. The preparation of ZnO nanoparticles in DMF results in their adhesion to the clean glass walls, which can be used as the cleanest method for depositing nanostructured ZnO thin films, by simply dipping. This synthesis method could be applied to other metallic carboxylate salts to form the corresponding nanostructured metal oxides. HR-TEM studies confirm the coexistence of ZnO nanocrystals with wurtzite and rock salt structures. The presence of ZnO rock salt NPs might be a consequence of a phase transformation induced by particle size and/or by the interaction of cyclohexanebutyrate−ZnO NPs.

Experimental Section

Materials. Zinc cyclohexanebutyrate dihydrate, $Zn(CHB)_2 \cdot 2H_2O$ (Strem) and zinc acetate dihydrate, $Zn(OAc)_2 \cdot 2H_2O$, (99.9%, Baker), were used in their commercial form without further purification. Dimethyl sulfoxide, DMSO (ACS, Sigma) and *N*,*N*′-dimethylformamide, DMF (99.9%, Baker) were dried over previously activated Linde 4 Å sieves at 500 °C for 16 h.[28] Ultrapure water (18 MΩcm^{-1}) was obtained from a Barnstead E-pure deionization system.

Synthesis Procedure. The synthesis of colloidal ZnO by the spontaneous hydrolysis of zinc carboxylate salt in DMSO (or DMF) requires 0.0044 g of $Zn(CHB)_2 \cdot 2H_2O$ (or 0.0022 g of $Zn(OAc)_2 \cdot 2H_2O$), which was dissolved in 50 mL of the anhydrous solvent (previously saturated with argon) in an Erlenmeyer flask to get a final concentration of 2×10^{-4} M. For the DMSO−H_2O and DMF−H_2O preparations, a fixed 3% of water by volume (1.5 mL) was added to the corresponding anhydrous solvent quantity (48.5 mL) before adding the carboxylate salt. Those experiments were performed with higher starting zinc salt concentration (1×10^{-3} M) in order to contrast better the optical responses between the different systems. Spectral measurements at 50 °C were performed using a Peltier thermocontrol system coupled to a holder cell of an electronic absorption spectrophotometer. Precipitate samples (from DMF) for X-ray diffraction measurements were separated from dispersions by centrifugation at 3500 rpm for 20 min, washed with acetone and dried at 40 °C. Thin films were prepared by dipping a well cleaned Corning glass plate in the pre-prepared solution of zinc acetate. All glassware was cleaned with moderately concentrated nitric acid and then washed with Alconox detergent and rinsed with plenty of ultrapure water.

Instruments. UV−vis absorption spectra were obtained by an Ocean Optics CHEM2000 fiber optic spectrophotometer coupled to a Hewlett-Packard Peltier thermocontrol system. Fluorescence spectra were collected on a modular Fluorolog 3 SPEX spectrofluorometer, fixing the excitation wavelength at 340 nm. High-resolution transmission electron microphotographs (HR-TEM) were obtained using a JEOL 4000-EX instrument, operating at 400 kV, by depositing a drop of the colloidal DMSO dispersion onto 200 mesh Cu grids coated with carbon/collodion layer. The particle size distribution was obtained from digitalized amplified micrographs by averaging the larger and smaller axis diameters measured in each particle. X-ray diffraction patterns were measured in a Siemens D5000 equipment using Cu Kα radiation. To determine the crystallite size, a peak broadening method was applied using the classical Scherrer−Warren equation[29] over the [102] and [210] reflections. Dynamic light scattering (DLS) measurements were collected using a HPPS Malvern nanoparticle sizer. Fast Fourier transform (FFT) of HR-TEM micrograph images was done by means of CRISP software[30] (version 1.7n).

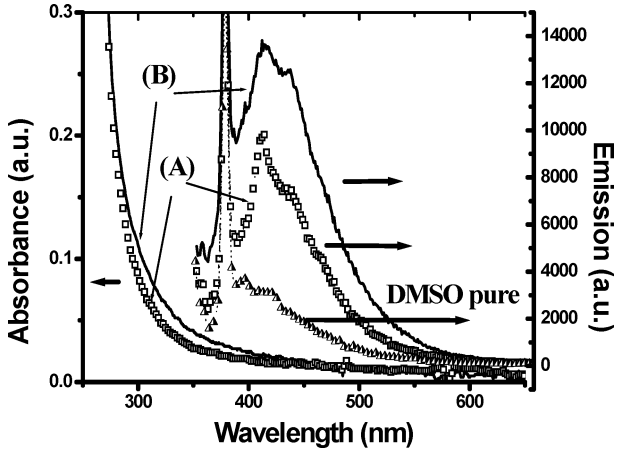

Figure 1. UV−visible electronic absorption and emission spectra of ZnO nanoparticles dispersed in DMSO prepared by the spontaneous hydrolysis of zinc cyclohexanebutyrate (2×10^{-4} M). (A) After 5 min, (B) after 20 min. For comparison, the DMSO emission spectrum also is shown.

Results and Discussion

DMSO Dispersions. In a previous work[31] we have shown the preparation of stable ZnO nanoparticle dispersions, using sodium hydroxide and zinc cyclohexanebutyrate in DMSO. Its UV−vis electronic absorption spectrum displays a band edge at 348 nm, which is shifted after 3 days toward 361 nm. Brus' model predicts a ZnO nanocrystal with diameter of 3.7 nm.

Later, during the preparations of ZnO colloids, we found that spontaneous hydrolysis of zinc carboxylate dihydrate salts (acetate and cyclohexanebutyrate) takes place in DMSO at room temperature (approximately 23 °C), leading to the formation of ZnO nanoparticles. Therefore, under these experimental conditions, it is not necessary to add any aqueous sodium hydroxide to obtain ZnO nanoclusters. For both carboxylates (2×10^{-4} M) and without the addition of water, the progress of the reaction can be observed only as a progressive increase in the emission spectra with time (see Figure 1 as an example). The emission spectrum shows the same two maxima, centered at 410 and 430 nm, as those obtained previously by the reaction of zinc acetate with sodium hydroxide in DMSO. The electronic absorption spectra show only a small displacement in the absorption edge of the solvent (near 300 nm), which probably is overlapping the absorption edge of ZnO nanoparticles. In this case, the mean particle size should be very small (<2.0 nm). Similar optical behavior had been previously reported for ZnO nanoparticles.[7,8,32] We cannot overlook that the reaction is still incomplete at this moment.

Our results suggest that the reaction rate depends proportionally on the temperature, zinc carboxylate concentration, and water content in DMSO. For example, at room temperature (ca. 23 °C) and low concentration (2×10^{-4} M), the reaction is very slow. It takes several days for stabilization of the optical response. So, for this reason, we decided to increase the temperature to 50 °C, and the reaction was completed in a period less than 30 min.

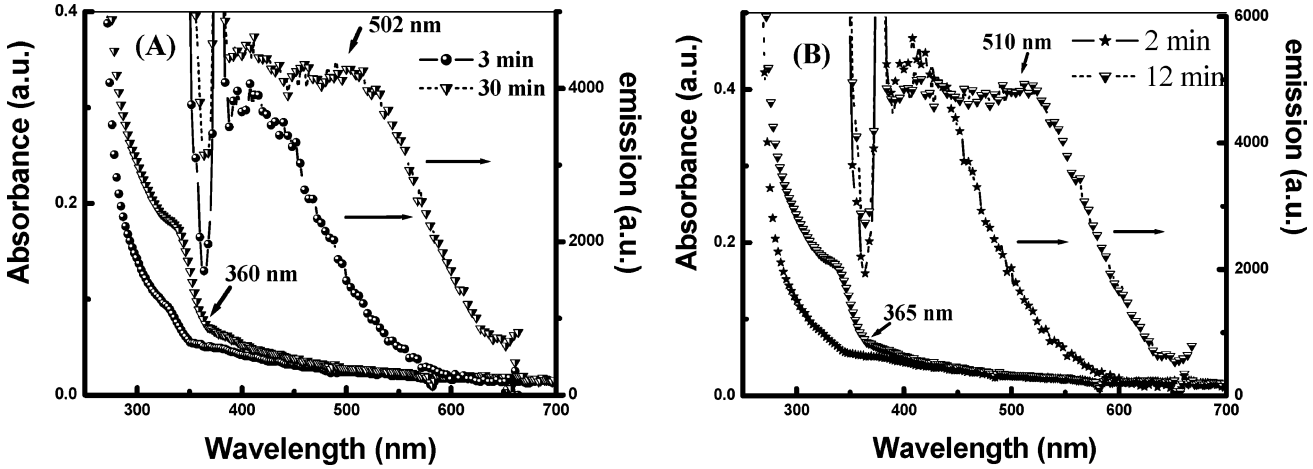

Figure 2. Electronic absorption and emission spectra of the hydrolysis of zinc carboxylate salts (2×10^{-4} M) in DMSO-3% of water, at 50 °C, at the beginning and at the end of the hydrolysis reaction. Left plot (A) shows the formation of ZnO nanoparticles from zinc cyclohexanebutyrate, and the right side plot (B) from zinc acetate. These dispersions are stable for two months.

It is necessary to control the concentration of water, since the hydrolysis reaction rate depends on this parameter. One has to be very careful since DMSO and DMF are highly hygroscopic in order to get reproducibility.

The water concentration was fixed at 3% in volume. This concentration guarantees complete hydrolysis for the following reasons. (i) The surface tension of the DMSO−H_2O mixtures increases with water content,[33] generating a higher equilibrium water concentration at the gas−liquid interface. This tends to minimize the water absorption from the environment. Therefore, synthesis reproducibility is assured. (ii) For this concentration, the basic character of this mixture remains very close to the solvent basicity for DMSO.[34] The basic properties of this reaction medium play a crucial role in the present synthesis procedure because it is the cornerstone in the hydrolysis mechanism, when it becomes the main source of hydroxyl anions, according to the following equilibrium:[35]

$$S_{(l)} + H-O-H_{(l)} \rightleftarrows [S-H]^+_{(solv)} + OH^-_{(solv)} \qquad (I)$$

where S = solvent (DMSO, DMF).

Similar considerations can be extended to DMF.[36−38] It can be stated that these polar−aprotic−solvent/water mixtures become an appropriate media for the hydrolysis reactions of different metals. Some of these hydrolytic media yield the corresponding metal oxide through a condensation route. Equilibrium (I) is the initial step that provides the hydroxyl anions required to form the zinc hydroxyl-species that turn into the primary entity for the subsequent propagation step of the condensation reaction,[39] which generates the metal oxide. The final condensation takes place through the elimination of the carboxylate moieties, which yield the well-known oligomeric tetracoordinated species (e.g., $Zn_4O(Ac)_6$),[10,40] the precursor of ZnO nanoparticles. It should be noted that water contribution from the carboxylate precursor is very small (7.2×10^{-4} % volume) when compared with 3% added H_2O, or sufficiently small to be neglected, in comparison with typical DMSO water impurities (10^{-2} %).

Figure 2 shows the electronic absorption and emission spectra (at the beginning and at the end of the each hydrolysis reaction of zinc carboxylate). It was assumed that hydrolysis reactions were completed when the absorption spectra remained unchanged. The graphics exhibit a rather similar optical behavior for the ZnO nanoparticles obtained from the different salts. The most remarkable feature among the samples is that those NPs obtained from CHB show a slightly blue shifted optical response in the electronic absorption and emission spectra with respect to NPs obtained from OAc. When anhydrous solvent is used for the hydrolysis reaction of both salts, it is easy to notice that the rate is controlled by absorption of water from the environment.

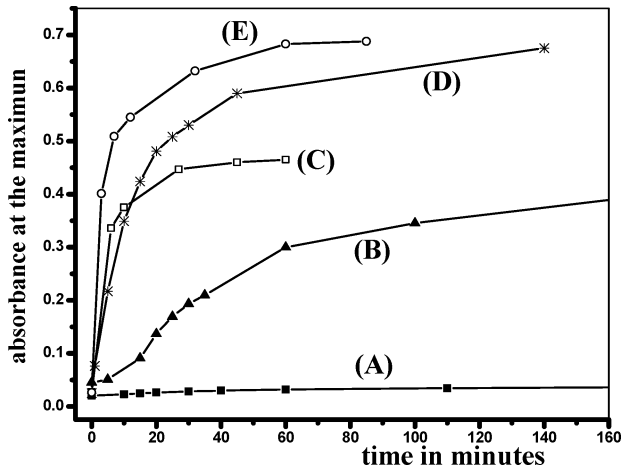

Figure 3. Absorbance maximum values vs time for the hydrolysis of zinc salts; $[Zn]_o = 1 \times 10^{-3}$ M. (A) $Zn(CHB)_2 \cdot 2H_2O$ in anhydrous DMSO and in a sealed vessel. (B) and (C) $Zn(CHB)_2 \cdot 2H_2O$ and $Zn(OAc)_2 \cdot 2H_2O$ respectively, in anhydrous DMSO and open container. (D) and (E) the same as in B and C, with 3% added H_2O to anhydrous DMSO. It should be mentioned that the absorbance maximum values were not taken at a fixed wavelength because the maximum shifts with the reaction progress, thus, these values correspond to the inflection point in the ZnO band appearing at wavelengths for which DMSO absorption is very small.

In Figure 3 the electronic absorbance maximum vs time is plotted, representing the reaction progress under different reaction conditions. The concentration for these experiments is increased up to 1×10^{-3} M, to boost the reaction rate, especially for those cases in which water is not present. This graph clearly provides evidence of the strong dependence on the water content. Compare this, for instance, to case (A) in which the reaction is carried out in a sealed vessel dissolving zinc cyclohexanebutyrate in anhydrous DMSO. Despite the reaction being very slow under these conditions, it takes place due to the fact that the zinc dihydrate salt acts as water source for hydrolysis. When the reaction is carried out in an open container, the hygroscopic solvent absorbs water from the surroundings, increasing the

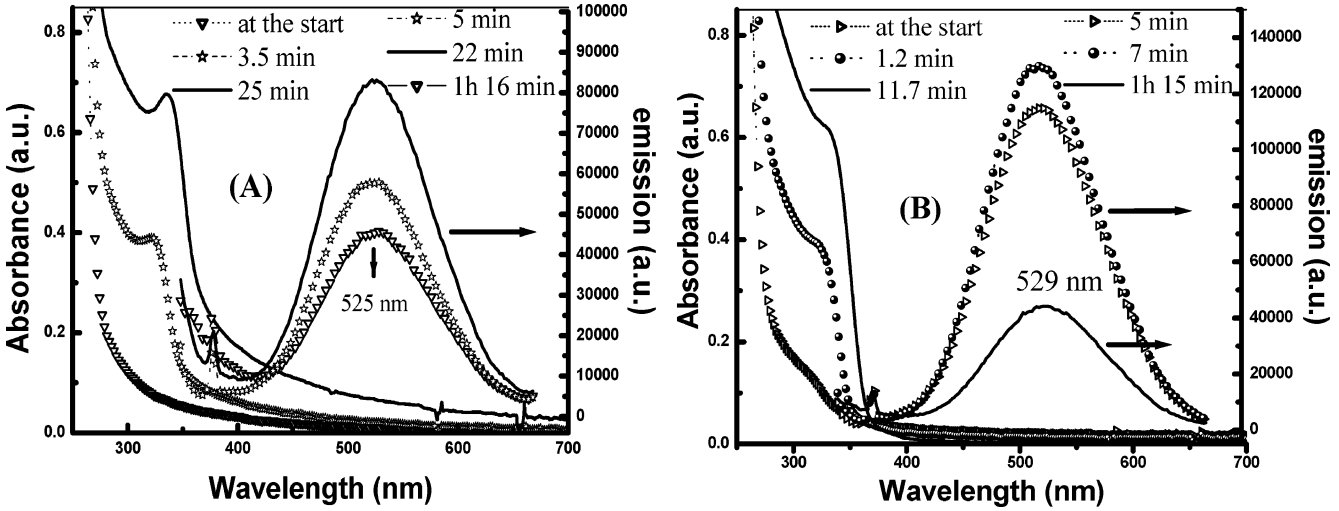

Figure 4. Time evolution of the optical response of ZnO nanoparticles, dispersed in DMSO-3% H_2O, at 50 °C. In both cases, the initial salt concentration is 1×10^{-3} M (A) obtained from $Zn(CHB)_2 \cdot 2H_2O$, (B) produced from $Zn(OAc)_2 \cdot 2H_2O$. Only few representative spectra of both samples had been displayed.

velocity of the hydrolysis of both carboxylates (compare (B) and/or (C) with (A) in Figure 3).

When water concentration is fixed, hydrolysis occurs in a faster way ((D) and (E) curves in Figure 3). In addition, it can be observed that, in all cases, the condensation process proceeds faster when acetate is used as carboxylate precursor. This implies that the carboxylate nature (composition, structure, hydrophobic surface, and especially the electron donor capacity) plays an important role in the reaction mechanism, modulating nucleation and/or the growth of the ZnO nanoparticles. The difference in reactivity between these two carboxylates can be attributed to the low electron donor capacity of the acetate anions in comparison with that of a large anion, such as CHB. For the latter, the local charge density at the carboxyl group is increased through electron injection from the σ molecular orbital (well-known in classic organic chemistry as +I effect).[41] Therefore, the interaction of cyclohexanebutyrate anions with Zn^{2+} is stronger and its dissociation more difficult during the propagation step of the condensation process.[39] Also, it can be viewed as a hindered OH^--nucleophilic attack toward Zn^{2+} due to higher electron donor capacity of CHB anion. The strong cyclohexanebutyrate moiety bonding to the surface Zn^{2+} cations also affects the Ostwald ripening process.

It is important to take into account that the dissociation constants of the majority of carboxylic acids, in DMSO and/or DMF, are lower than those in aqueous solutions, especially for those acids containing large aliphatic chains.[42−44]

Figure 4, shows the time evolution of the optical response of ZnO nanoparticles (A) obtained from zinc cyclohexanebutyrate (1×10^{-3} M) and (B) obtained from zinc acetate (1×10^{-3} M); both in DMSO 3% H_2O, at 50 °C. The increase of the absorbance at the maximum and the shift of the electronic absorption onset (λ_{onset}) in each sample indicate the simultaneous process of nucleation and growing of the particle size distribution. Emission spectra of both samples display the typical green emission band of ZnO, centered at 525 nm for the CHB salt and at 529 nm for OAc. The final intensity values are reasonably similar. It is remarkable that although the intensities of electronic absorption spectra remain stable, the emission intensity gradually decrease, which probably is related to equilibrium modifications at the surface of the NPs.[33,45] Another noticeable feature of the emission spectra of these samples is that, for the same concentration (1×10^{-3} M), absorption onset of the nanoparticles obtained from $Zn(CHB)_2 \cdot 2H_2O$ shows a long-wave tail, which is usually associated with a sub-bandgap phonon assisted optical transition. Zou[46] et al., have demonstrated that this spectral behavior is related to the optical response of the ZnO crystallized in the rock salt structure, previously predicted by Jaffe et al.[47] Later, in this paper, direct evidence of the presence of ZnO NPs with rock salt structure in the above-mentioned samples will be provided from the HR-TEM images. However, we do not discard the possibility that the absorption spectrum long wave tail could also be related to structural surface-disorder, resulting from the strong interaction between ZnO and CHB anions. It should be noted that ZnO colloidal dispersions at a concentration (1×10^{-3} M) in DMSO are not very stable, regardless of the starting salt. Precipitation takes place after 2 days. Also, it is very important to stress the fact that for high water content (> 30%, water molar fraction $X_w \geq 0.65$) the hydrolysis and condensation processes to obtain ZnO from CHB and OAc carboxylates in DMSO does not proceed. In the first case, the reaction is limited by the low solubility of the CHB salt in the water−DMSO mixture. Probably, in the acetate case the reason is a thermodynamics limitation ($\Delta G_f°$ of ZnO through condensation in water is near zero).[48] Catalan et al.[34] had demonstrated that, when $X_w \geq 0.65$, the mixture tends to behave as water (i.e., medium becomes substantially acidic).

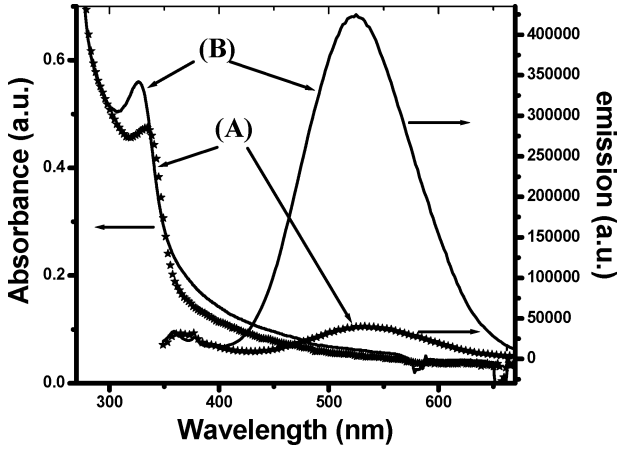

Figure 5. Electronic absorption and emission spectra of ZnO nanoparticles (A) obtained from $Zn(OAc)_2 \cdot 2H_2O$ and (B) synthesized from $Zn(CHB)_2 \cdot 2H_2O$. In both cases the salt concentration is 1×10^{-3} M, in DMF-3% H_2O at $T = 50$ °C.

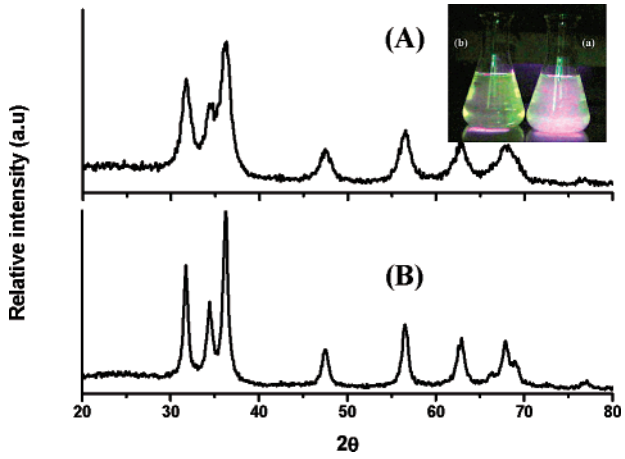

Figure 6. X-ray diffraction patterns of the ZnO nanocrystallites obtained from (A) $Zn(CHB)_2 \cdot 2H_2O$ and (B) $Zn(OAc)_2 \cdot 2H_2O$. Both zinc salts (1×10^{-3} M) were dissolved in DMF, with 3% of water, and then heated during 1.5 h under vigorous stirring, at 50 °C, to obtain a precipitate. The right-hand photograph shows the green emission differences between the samples used for X-ray experiments (illuminated under low intensity UV lamp $\lambda = 362$ nm).

Furthermore, any trial to obtain ZnO nanoparticles from zinc chloride, in DMSO, was unsuccessful, revealing the importance of the use of a carboxylate as starting salt.

DMF Dispersions. The same procedure used to obtain ZnO nanoparticles in DMSO was used for the DMF preparations. Figure 5 shows the behavior of zinc carboxylate salts in DMF. The displayed electronic absorption and emission spectra are those for each salt hydrolysis after reaching the maximum of the optical response. In this case, the electronic absorption spectra of these zinc carboxylates are quite similar, except that as in DMSO the zinc acetate hydrolysis is more favored occurring in a shorter period.

It is important to point out that for this concentration, 1×10^{-3} M, the ZnO nanoparticle dispersions obtained in DMF, are not stable and readily precipitate after 1.0 h. Precipitation of both systems under same conditions and at same time allows the comparison of ZnO particle size, in order to explain the main features electronic absorption and emission optical response. Besides, the emission intensity is much higher for ZnO obtained from cyclohexanebutyrate, indicating that probably the concentration of emitting species (ZnO nanoparticles) is higher.

For any concentration, in the range 2×10^{-4} M up to 2.5×10^{-3} M, and under the same reaction conditions, the absorption edge for the ZnO colloids obtained from the CHB salt always has a red shift, in comparison with the spectra of those from zinc acetate salt.

This can be interpreted as a larger particle size. However, the fluorescence spectra for these ZnO dispersions show that the exciton and visible emission of ZnO−CHB NPs appear blue shifted in comparison with ZnO−OAc nanoparticles. This result is contrary to the information from the absorption spectra.

To clarify this apparent contradiction, which also arises for the DMSO dispersions, both types of ZnO nanocrystallites (from acetate and CHB) were precipitated from DMF (zinc salt concentration, 1×10^{-3} M). The resulting powders were studied by X-ray diffraction spectroscopy. Figure 6 shows the corresponding X-ray diffraction patterns of both samples. All reflections are in agreement with the hexagonal ZnO wurtzite phase structure. Thermogravimetric analyses show that these samples are contaminated with carboxylate residues, which are not seen using X-ray diffraction or HR-TEM, probably due to the fact that they are absorbed onto the nanoparticles surface, thus having only a short range of structural order. The peak broadenings clearly show that the mean particle size is smaller for the ZnO−CHB nanoparticles. By application of the Scherrer−Warren equation, the calculated average crystallite sizes are 4.8 and 7.1 nm for the ZnO nanoparticles, obtained from CHB and acetate salts, respectively. Therefore, the long tail spectrum and the red shifted wavelength absorption edge for the CHB capped ZnO nanoparticles do not necessarily signify that the average particle size is larger than those obtained from the zinc acetate salt.

HR-TEM Analysis. The HR-TEM images were collected 20 days after preparation to ensure the stability of the dispersion. As expected, the examined samples contained crystalline ZnO. Figure 7 shows a selected HR-TEM image of ZnO−CHB nanocrystallites. Calculated d_{hkl} agrees well with the reported value for the wurtzite (hexagonal) structure of the stable ZnO macrocrystalline phase. By counting over 50 particles, we were able to obtain the particle size distribution shown in Figure 7. Large lumps, probably formed during the HR-TEM sample preparation, were not considered. Additionally, during the examination of the HR-TEM images of ZnO nanoparticles obtained from zinc cyclohexanebutyrate, we found a small

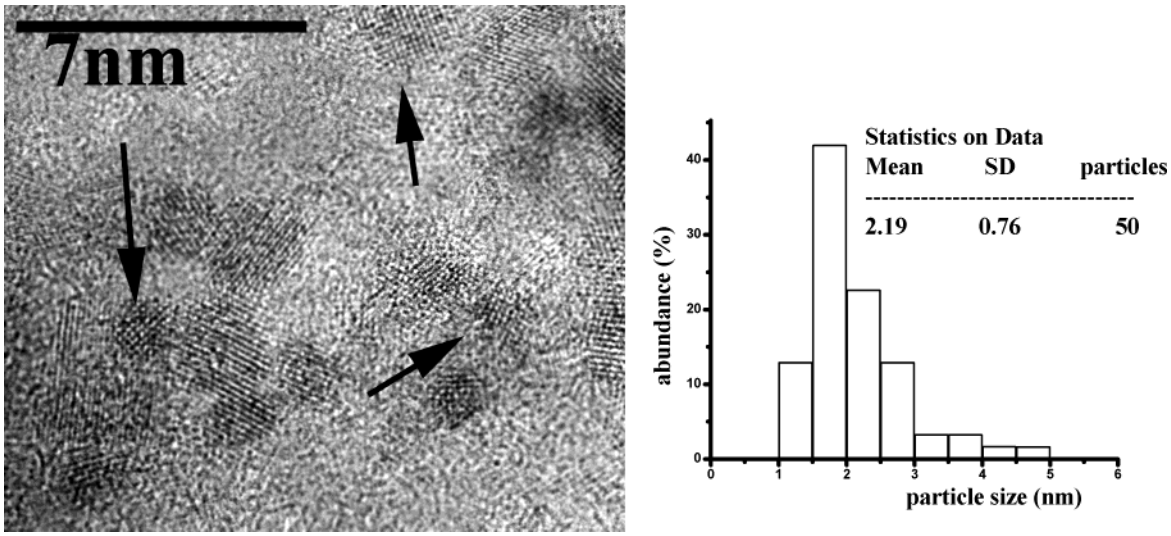

Figure 7. HR-TEM micrograph of ZnO nanoparticles (after 20 days) prepared from the spontaneous hydrolysis of zinc cyclohexanebutyrate (2×10^{-4} M) in DMSO-3% water, heated during 30 min at 50 °C, under vigorous stirring. The arrows point out some nanoparticles with cubic atomic arrangement. The plot shows the particle size distribution histogram of capped CHB−ZnO nanoparticles.

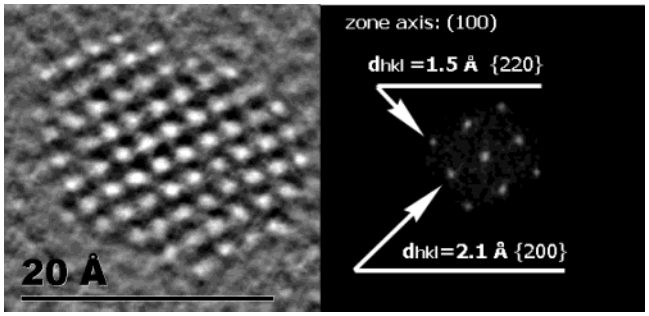

Figure 8. HR-TEM micrograph of a ZnO nanoparticle with cubic rock salt structure in a 200 plane projection. This sample was obtained from the hydrolysis of zinc cyclohexanebutyrate (2×10^{-4} M) in DMSO-3% H_2O, and heating at 50 °C for 12 min. At the right FFT of the micrograph with calculated d_{hkl}.

quantity (approximately 5%) of particles that show atomic arrangements, which do not correspond to the wurtzite structure, see Figures 7 and 8. For this ZnO NP, the calculated d_{hkl} from an FFT image of a magnified nanoparticle micrograph corresponds to the interplanar distance of ZnO with rock salt structure, which is known as a metastable allotropic phase of this metal oxide.[49] It can be obtained by applying a relatively modest hydrostatic pressure (8.5 GPa) to ZnO wurtzite structure.

The differences in free energy between the ZnO phases (Figure 9) suggest the simultaneous presence of ZnO wurtzite and zinc blende, and seldom the rock salt structure. This means that the presence of this phase is probably related to an induced phase transition due to particle size and the interaction ZnO−CHB. Dua et al. have claimed that the phase transition in $Bi_4Ti_3O_{12}$ solid is a consequence of the size diminishment.[50] However, other authors suggest that the zinc blend semiconductors prefer a cubic structure due to size or to surface modifier interaction.[51,52] Since indirect band gap transitions of the ZnO with rock salt structure may occur,[46,47] they can be partly responsible for the optical behavior of ZnO NPs obtained from CHB salt.

HR-TEM images of the acetate-capped ZnO NPs show the presence of unique well faceted nanocrystals with wurtzite structure (see Figure 9A, B, and C). The particle size abundance

SCHEME 1: Schematic Representation of the Crystal Structures of the Different Allotropic Forms of ZnO, and the Differences in ΔG_f.

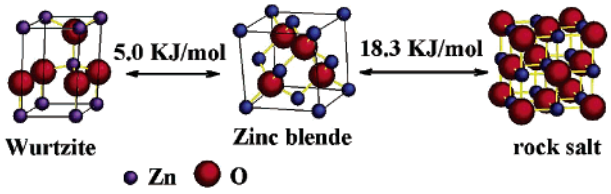

plot exhibits a narrower distribution with a mean particle size slightly larger in comparison to the CHB-capped ZnO case. In this case, the calculated d_{hkl} also agrees well with those values reported for wurtzite−ZnO.

It is important to stress that particles with rock salt or a structure different from wurtzite were not found in this ZnO−AcO sample. This probably indicates that its presence is conditioned either to a size effect or to a capping effect of the CHB moieties, or, most likely, to both.

Dynamic Light Scattering Measurements. Figure 10 shows the particle size distribution for ZnO nanoparticles synthesized from $Zn(CHB)_2 \cdot 2H_2O$ and $Zn(OAc)_2 \cdot 2H_2O$. In both cases, the zinc salt concentration is 2×10^{-4} M, solved in DMSO-3% H_2O and heating at 50 °C. As can be seen, ZnO nanoparticles from CHB salt present two particle size distributions; the first population peaks at 4.8 nm (integral intensity = 14%) and the second one at 3.8 μm (integral intensity = 84%). It should be remarked that intensity (%) does not represent the amount of mass contributing to each peak. The amount of light scattered is proportional to the molecular mass, and the molecular mass increases as R^3 (R = hydrodynamic radius of the particle). Therefore, the second particle size distribution, which includes agglomerates of nanocrystals, could correspond to a small mass quantity of ZnO. In the case of the ZnO−OAc dispersions, only one particle size distribution is present with an average size of 55.2 nm.

In this case, the dispersion appears to be formed only by agglomerates of nanocrystals with one distribution. These results are a clear direct evidence of the capping action of CHB anions,

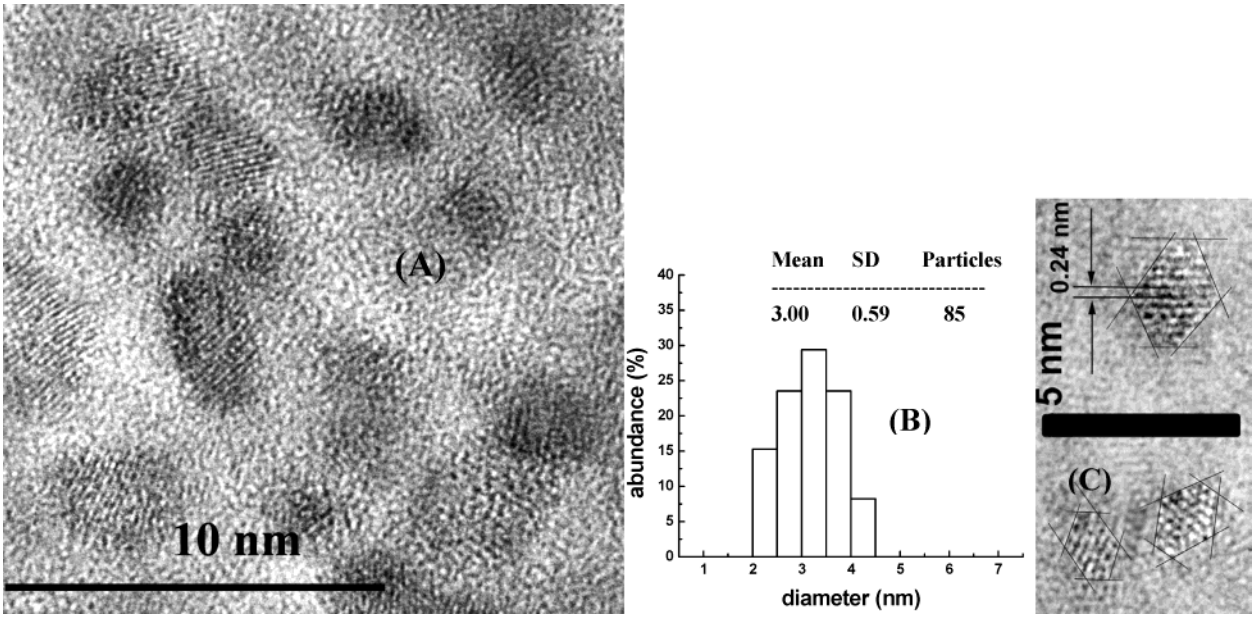

Figure 9. (A) HR-TEM micrographs of ZnO nanoparticles (after 20 days) obtained from the spontaneous hydrolysis of zinc acetate (2×10^{-4} M) in DMSO-3% water and then heated during 12 min at 50 °C under vigorous stirring. Plot (B) is the resulting particle size distribution histogram of this ZnO nanocrystallite dispersion. (C) Well faceted nanocrystallites of ZnO from the same sample.

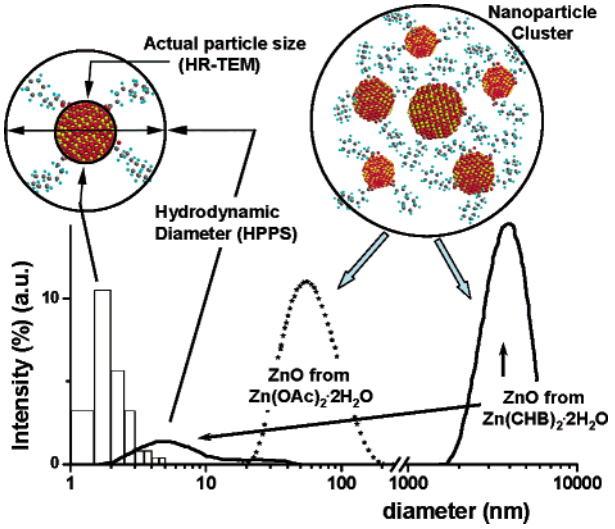

Figure 10. Dynamic light scattering measurements of particle size distribution of ZnO (2×10^{-4} M) dispersions in DMSO-3% H_2O, and heating at 50 °C. Continuous and dotted lines correspond to ZnO NPs generated from $Zn(CHB)_2 \cdot 2H_2O$ and $Zn(OAc)_2 \cdot 2H_2O$, respectively. Bars represent the HR-TEM particle size distribution measured for ZnO−CHB NPs (produced under the same experimental conditions) for comparison with DLS measurements.

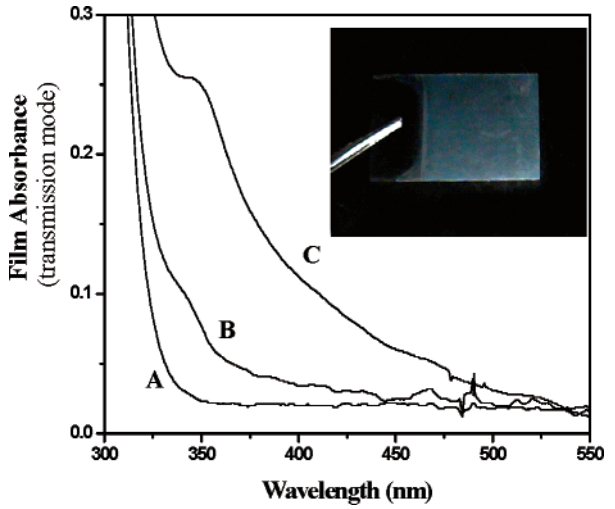

Figure 11. The photograph inset shows a chemical bath deposited thin film obtained from a ZnO−OAc nanoparticle dispersion in DMF; (2.5×10^{-3} M), $T = 50$ °C. The Corning glass substrate dimensions are 24×30 mm. Plot shows the electronic absorption spectra of: (A) clean glass substrate, (B) Glass substrate after an immersion into the ZnO−AcO nanoparticle DMF dispersion, during 20 min, (C) Glass substrate after an immersion during 1 h on the same ZnO dispersion.

which prevents the agglomeration. It is also important to note that the particle size distribution derived from light scattering measurements agrees with that obtained from HR-TEM observations; considering that the first measurements do not represent the real semiconductor particle size, just a hydrodynamic diameter distribution. The upper part, (left) in Figure 10, is a schematic representation that explains the phenomenological situation in the first section of the DLS and HR-TEM particle size distributions. The upper part, (right) of the same figure, illustrates the corresponding formation of nanoparticle agglomerates in both samples. Consequently, the existence of these huge agglomerates of nanoparticles (with hydrodynamic diameter around 3.8 μm) in the case of ZnO−CHB NPs can also considerably contribute to the light dispersion in the electronic absorption spectra, leading to long-wave tails.[53] Therefore, we cannot overlook that long-wave tails present in the spectra of ZnO−CHB NPs (especially for more concentrated samples (1×10^{-3} M)) are the result of light scattering from agglomerates.

ZnO Film Deposition. We had found that the nanoparticles from ZnO dispersions in DMF tend to adhere to the glassware and UV cell walls. This phenomenon has also been earlier noted by Liz-Marzán et al., who observed that when silver nitrate is reduced by DMF, the metallic particles also tend to adhere to the glass walls.[54,55]

After 20 min of immersion of a glass piece into the dispersion, a film of ZnO nanoparticles is deposited, displaying a $\lambda_{onset} = 360$ nm in transmission mode, Figure 11. This means that the obtained film is formed by nanoparticles that still show the confinement effect (i.e., the particle size is under 7 nm).

Conclusions

We found a new, clean, reproducible, and direct method for the synthesis of zinc oxide nanoparticles. Stable ZnO nanoparticle dispersions with average diameter close to 2 nm and narrow size distributions can be prepared by simple addition of a zinc carboxylate to DMSO or DMF. It is important to stress that it is not necessary to add water to DMSO or DMF in order to obtain ZnO nanoparticles from a zinc carboxylate; it is only necessary to fix the water composition if reproducible results are desired.

HR-TEM, X-ray powder diffraction and DLS characterizations of ZnO nanoparticles, obtained in DMSO and DMF, clearly show that the cyclohexanebutyrate anion appears to be a more effective capping agent than acetate. A direct evidence of ZnO NPs with rock salt structure synthesized in DMSO is shown. This type of NPs is not present when zinc acetate is used as starting salt.

When DMF is used as solvent, the synthesis of ZnO nanoparticles from the carboxylate salt becomes a good alternative and very easy pathway to obtain films of this semiconductor, deposited onto glass substrates. The present synthesis pathway could be generalized to other transition metals allowing the preparation of the corresponding metal oxide nanoclusters. The hydrolysis process of several metallic cations, such as Cd(II) and Ti(IV), is still under intensive research in our group.

Acknowledgment. Thanks to K. Mattison from Malvern for the dynamic light scattering size measurements. We thank Dr. A. Vázquez-Olmos from CCADET-UNAM, Dr. S. E. Castillo-Blum and Prof. E. Zeller from FQUNAM, Dr. V. Basiuk from IINUNAM, and O. Jiménez from CINVESTAV-Qro for their useful discussions and suggestions to this work. This work was partially supported by CONACyT (project E-130) and DGAPA-UNAM (projects: IN100398 & IN107700). G.R.G. thanks DGEP-UNAM for the scholarship.

References and Notes

(1) Sang, B.; Konagai, M. *Jpn. J. Appl. Phys.* **1996**, *35*, 602.
(2) Villasenor, J.; Mansilla, H. D. *J. Photochem. Photobiol. A: Chem.* **1996**, *93*, 205.
(3) Bahadur, L.; Rao, N. T. *J. Photochem. Photobiol. A: Chem.* **1995**, *91*, 233.
(4) Hu, Z.; Chen, S.; Peng, S. *J. Colloid Interface Sci.* **1996**, *182*, 457.
(5) Chopra, K. L.; Das, S. R. *Thin Solid Films* **1983**, *102*, 1.
(6) Bagnall, D. M.; Chen, Y. F.; Zhu, Z.; Yao, T.; Koyama, S.; Shen, M. Y.; Goto, T. *Appl. Phys. Lett.* **1997**, *70*(17), 2230.
(7) Bahnemann, D. W.; Kormann, C.; Hoffmann, M. R. *J. Phys. Chem.* **1987**, *91*, 3789.
(8) Spanhel, L.; Anderson, M. A. *J. Am. Chem. Soc.* **1991**, *113*, 2833.
(9) Hu, Z.; Chen, S.; Peng, S. *J. Colloid Interface Sci.* **1996**, *182*, 457.
(10) Inubushi, Y.; Takami, R.; Iwasaki, M.; Tada, H.; Ito, S. *J. Colloid Interface Sci.* **1998**, *200*, 220.

(11) Guo, L.; Yang, S.; Yang, C.; Yu, P.; Wang, J.; Ge, W.; Wong, G. K. L. *Appl. Phys. Lett.* **2000**, *76*, 2901.
(12) Carnes, C. L.; Klabunde, K. J. *Langmuir* **2000**, *16*, 3764.
(13) Kobayashi, K.; Matsubara, T.; Matsushima, S.; Shirakata, S.; Isomura, S.; Okada, G. *Thin Solid Films* **1995**, *266*, 106.
(14) Audebrand, N.; Auffrédic, J.-P.; Louër, D. *Chem. Mater.* **1998**, *10*, 2450.
(15) Studenikin, S. A.; Golego, N.; Cocivera, M. *J. Appl. Phys.* **1998**, *83*, 2104.
(16) Wu, R.; Xie, C.; Xia, H.; Hu, J.; Wang, A. *J. Cryst. Growth* **2000**, *217*, 274.
(17) Meulenkamp, E. A. *J. Phys. Chem. B* **1998**, *102*, 7764.
(18) Steiner, E. C.; Gilbert, J. M. *J. Am. Chem. Soc.* **1965**, *87*, 382.
(19) Parker, A. J. In *Advances in Organic Chemistry*; Raphael, R. A., Taylor, E. C., Wynnberg, H., Eds.; Wiley-Interscience: New York, 1965; pp 1−46.
(20) McGarry, F. P.; Jockusch, S.; Fujiwara, Y.; Kaprinidis, Nikolas, A.; Turro, J. N. *J. Phys. Chem. A* **1997**, *101*, 764.
(21) Ivy, L. R.; Hafez, M. A.; Abelt, J. C. *J. Org. Chem.* **1997**, *62*, 6415.
(22) Díaz, D.; Rivera, M.; Tong, Ni; Rodríguez, J. C.; Castillo-Blum, S. E.; Nagesha, D.; Robles, J.; Alvarez-Fregoso, O. J.; Kotov, N. A. *J. Phys. Chem. B* **1999**, *103*, 9854.
(23) Kanemoto, M.; Ishihara, K.; Wada, Y.; Sakata, T.; Mori, H.; Yanagida, S. *Chem. Lett.* **1992**, 835.
(24) Kanemoto, M.; Hosokawa, H.; Wada, Y.; Murakoshi, K.; Yanagida, S.; Sakata, T.; Mori, H.; Ishikawa, M.; Kobayashi, H. *J. Chem. Soc., Faraday Trans.* **1996**, *92*, 2401.
(25) Fujiwara, H.; Hosokawa, H.; Murakoshi, K.; Wada, Y.; Yanagida, S.; Okada, T.; Kobayashi, H. *J. Phys. Chem. B* **1997**, *101*, 8270.
(26) Rodríguez-Gattorno, G.; Díaz, D.; Rendón, L.; Hernández-Segura, G. O. *J. Phys. Chem. B* **2002**, *106*, 2482.
(27) Elbaum, R.; Vega, S.; Hodes, G. *Chem. Mater.* **2001**, *13*, 2272.
(28) Kissinger, P. T.; Heineman, W. R. *Laboratory Techniques in Electroanalytical Chemistry*; Marcel Dekker: New York, 1984; p 377.
(29) Klug, H. P.; Alexander, L. E. *X-ray Diffraction Procedures for Polycrystalline and Amorphous Materials;* John Wiley & Sons: New York, 1974; p 687.
(30) Hovmöffer, S. *Ultramicroscopy* **1992**, *41*, 121.
(31) Németh, J.; Rodríguez-Gattorno, G.; Vázquez-Olmos, A. R.; Rendón-Vázquez, L.; Díaz, D.; Dékány I. *Colloidal Dispersions of ZnO Nanoparticles and Layered Silicates in DMSO Medium*. Manuscript in preparation.
(32) Monticone, S.; Tufeu, R.; Kanaev, A. V. *J. Phys. Chem. B* **1998**, *102*, 2854.
(33) Kenttämaa, J.; Lindberg, J. J. *Suom. Kemistil. B* **1960**, *33*, 98.
(34) Catalán, J.; Díaz, C.; García-Blanco, F. *J. Org. Chem.* **2001**, *66*, 5846.
(35) Calligaris, M.; Carugo, O. *Coord. Chem. Rev.* **1996**, *153*, 83.
(36) Garcia, B.; Alcalde, R.; Leal, J. M.; Matos, J. S. *J. Chem. Soc., Faraday Trans.* **1997**, *93*, 1115.
(37) Visser, C.; Somsen, G. *J. Phys. Chem.* **1974**, *78*, 1719.
(38) Rajasekhar, P.; Reddy, K. S. *Thermochim. Acta* **1987**, *17*, 379.
(39) Jolivet, J. P.; Henry, M.; Bescher, E. *Metal Oxides Chemistry and Synthesis. From Solution to Solid State;* John Wiley & Sons Ltd: U.K., 2001; p 25.
(40) Tokumoto, M. S.; Briois, V.; Santilli, C. V.; Pulcinelli, S. H. *J. Sol-Gel Sci. Technol.* **2003**, *26*, 547.
(41) Wingrove, A. S.; Caret, R. L. *Organic Chemistry*; Harper & Row: New York, 1981; p 135.
(42) Bordwell, F. G. *Acc. Chem. Res.* **1988**, *21*, 456.
(43) Mukerjee, P.; Ostrow, J. D. *Tetrahedron Lett.* **1998**, *39*, 423.
(44) Bordwell, F. G.; Branca, J. C.; Hughes, D. L.; Olmstead, W. N. *J. Org. Chem.* **1980**, *45*, 3305.
(45) Wong, Eva M.; Hoertz, P. G.; Liang, C. J.; Shi, B.-M.; Meyer, G. J.; Searson, P. C. *Langmuir* **2001**, *17*, 8362.
(46) Zou, B. S.; Volkov, V. V.; Wang, Z. L. *Chem. Mater.* **1999**, *11*, 3037.
(47) Jaffe, J. E.; Pandey, R.; Kunz, A. B. *Phys. Rev. B* **1991**, *43*, 14030.
(48) Weast, R. C.; Astle, M. J.; Beyer, W. H. *CRC Handbook of Chemistry and Physics*, CRC Press: Boca Raton, FL, 1985; *66*, p D-92.
(49) Bates, C. H.; White, W. B.; Roy, R. *Science* **1962**, *137*, 993.
(50) Dua, Y. L.; Zhanga, M. S.; Chena, Q.; Yuana, Z. R.; Yina, Z.; Zhangb, Q. A. *Solid State Commun.* **2002,** *124*, 113.
(51) Bandaranayake, R.; Wen, G.; Lin, J.; Jiang, H.; Sorensen, C. *Appl. Phys. Lett.* **1995**, *67*, 831.
(52) Murakoshi, K.; Hosokawa, H.; Tanaka, N.; Saito, M.; Wada, Y.; Sakata, T.; Mori, H.; Yanagida, S. *Chem. Commun.* **1998**, *3*, 321.
(53) van de Hulst, H. C. *Light Scattering by Small Particles*; Dover Publications: New York, 1981; Part II.
(54) Pastoriza-Santos, I.; Liz-Marzan, L. M. *Langmuir* **1999**, *15*, 948.
(55) Pastoriza-Santos, I.; Serra-Rodríguez, C.; Liz-Marzán; L. M. *J. Colloid Interface Sci.* **2000,** *221*, 236.